Biosensors and Bioelectronics 26 (2011) 3227–3232

Contents lists available at ScienceDirect

Biosensors and Bioelectronics

journal homepage: www.elsevier.com/locate/bios

$[C_3(OH)_2mim][BF_4]$-Au/Pt biosensor for glutamate sensing *in vivo* integrated with on-line microdialysis system

Yanyan Yu[a], Xiaoqian Liu[a], Dawei Jiang[a], Qian Sun[a], Tianshu Zhou[b], Min Zhu[a], Litong Jin[a], Guoyue Shi[a,*]

[a] *Department of Chemistry and Shanghai Key Laboratory of Green Chemistry and Chemical Process, East China Normal University, 3663 Zhongshan Road(N), Shanghai, 200062, PR China*
[b] *Department of Environmental Science, East China Normal University, 3663 Zhongshan Road(N), Shanghai, 200062, PR China*

ARTICLE INFO

Article history:
Received 26 October 2010
Received in revised form
13 December 2010
Accepted 16 December 2010
Available online 23 December 2010

Keywords:
On-line microdialysis system
$[C_3(OH)_2mim][BF_4]$-Au/Pt nanocomposite
Glutamate biosensor
In vivo

ABSTRACT

A new type of hydroxyl functionalized room temperature ionic liquid (RTIL), $[C_3(OH)_2mim][BF_4]$, was synthesized herein and a novel H_2O_2 biosensor is fabricated with $[C_3(OH)_2mim][BF_4]$ as the substrate and electrodepositing bimetallic Au/Pt nanoparticles (NPs) onto the $[C_3(OH)_2mim][BF_4]$ film. The functionalization of RTIL with hydroxyl groups provided an appropriate environment for the preparation of more uniform and smaller Au/Pt NPs with the diameter of 2.5 nm ± 0.2 nm. Immobilized with glutamate oxidase (GlutaOx), the resulting GlutaOx-$[C_3(OH)_2mim][BF_4]$-Au/Pt-Nafion biosensor displayed excellent electrocatalytic response to glutamate at a potential of −200 mV. An effective on-line microdialysis system, which was powered by a microdialysis pump, was set up and used for the detection of glutamate successively in the striatum of rats. The glutamate biosensor in on-line microdialysis system showed good linear range from 0.5 μM to 20.0 μM with the detection limit of 0.17 μM (S/N = 3). The basal level of glutamate in the striatum of anaesthetic rats was calculated to be 3.01 ± 0.67 μM (n = 3). The application of the GlutaOx-$[C_3(OH)_2mim][BF_4]$-Au/Pt-Nafion electrode is further demonstrated for *in vivo* sensing of the variation of glutamate level in the striatum when rats received intraperitoneal (i.p.) injection of 100 mM KCl and brain electrical stimulation of the subthalamic nucleus area (STN). Both of the two kinds of stimulation resulted in an increase in the extracellular concentration of glutamate. This method has proved to be sensitive and reproducible, which enables its promising application in physiology and pathology.

1. Introduction

As one of the most important excitatory neurotransmitters in the central nervous system (CNS), glutamate has played a significant role in many aspects of brain functioning, such as, in cognitive processes and in the development and plasticity of CNS (Oldenziel et al., 2006a,b). It is also involved in the process of mediating energy expenditure, insulin–glucose homeostasis, the sleep–awake cycle, and the neuroendocrine output of the pituitary gland in the ventromedial hypothalamus (Tong et al., 2007; Wilson and Johnson, 2008). Since neuronal pathways in brain that use glutamate as a transmitter are heavily implicated in many neurological disorders, such as Schizophrenia, Parkinson's disease and Epilepsy, precise and real-time monitoring of glutamate level in the extracellular space of brain tissue would contribute significantly to the fundamental understanding of the role of glutamate in these disorders (Kulagina et al., 1999; Grace, 1991; Klockgether and Turski, 1993). The task is actually full of challenge because the concentration of glutamate in extracellular space is in the range of 4–350 μM (Chakraborty and Raj, 2007; Hu et al., 1994), far below that of AA, which exists at high concentrations (100–500 μM) in the brain (Weite et al., 2005), becoming the biggest interference in the detection of glutamate. Compared with spectrophotometric, fluorimetric and chromatographic methods (Jeffries et al., 1997), the employment of an electrochemical enzymatic biosensor has been proved to be a suitable approach for the detection of glutamate and has been widely used with microdialysis technique (Mao and Yamamoto, 2000; Niwa et al., 1997). Due to its short analytical time, high sensitivity and specificity to provide near real-time measurements, microdialysis sampling could provide us both the temporal and chemical information that we need to fully elucidate the biochemical processes (Hogant and Lunte, 1994).

Metal nanoparticles (NPs) have been proved a promising material for developing enzyme biosensors since they have different physical properties from bulk materials, such as, the quantum size effects and increased photochemical activity because of the high surface/volume ratio and unusual electronic properties of NPs (Tian et al., 2006; Daniel and Astruc, 2004). It has been well-known

* Corresponding author. Tel.: +86 21 62237105; fax: +86 21 62237105.
E-mail addresses: gyshi@chem.ecnu.edu.cn, iamshgy@hotmail.com (G. Shi).

0956-5663/$ – see front matter © 2010 Elsevier B.V. All rights reserved.
doi:10.1016/j.bios.2010.12.031

that the performance of metal NPs catalysts largely depends on their morphology, size and composition. Thus, great efforts have been attempted to realize both the size and morphology tunable synthesis of metal NPs. Recent results suggest that room temperature ionic liquids (RTILs) can be the preferable solvents in the synthesis and modification of nanostructured materials because of their unique properties, for example, the existence of extended hydrogen bonding, good thermal stability and high ionic conductivity (Howlett et al., 2004; Wang et al., 2003). It is believed that RTIL can limit diffusion of the NPs and thus promote formation of smaller particles (Brauer et al., 2001; Kottsieper et al., 2001). By tuning the RTILs' composition, the stability, size, and solubility of the NPs may all be tuned (Astruc et al., 2005). There has been great interest in the electrodeposition of metals from RTILs but this has largely involved the air and moisture sensitive chloroaluminate ionic liquids (Whitehead et al., 2004). Currently, it is becoming increasingly apparent that incorporation of functional groups into RTIL is indispensable as the functional groups can increase catalyst stability and/or improve catalyst retention (Fei et al., 2007). Different functional groups such as $-NH_2$, $-SH$, $-OH$, $-SO_3H$, etc. have been extensively attached to alkyl side chains on the imidazolium, pyridinium etc. cations (Zhang et al., 2007). The incorporation of such functional groups has made the RTILs more flexible to tune their physiochemical properties according to a specific application. Besides that, a number of critical aspects of RTILs make them an interesting medium in which enzymes and even living cells can retain their bioactivities, which provide us a facile way for the preparation of new biosensors (Maciej et al., 2006).

A few papers have reported the synthesis and catalytic application of composites of metal NPs and RTILs. Dupont et al. (2002) have reported an activated iridium NPs catalyst in $[C_4mim][PF_6]$ with an average diameter of 2–2.5 nm, which showed an obviously improved activity for the biophasic hydrogenation of various olefins and arenes. Other noble metal NPs catalysts such as gold and platinum NPs with tunable sizes synthesized in various imidazolium derivatives also exhibited remarkably high stability in aqueous solutions (Kim et al., 2004; Itoh et al., 2004). In our present work, we reported a newly synthesized RTIL, $[C_3(OH)_2mim][BF_4]$, which was characterized with two hydroxyl functionalities in the imidazolium core. It was found that the introduction of a functional group into an RTIL greatly improves its ability to stabilize Au/Pt alloy NPs with the size of $2.5\,nm \pm 0.2\,nm$. The existence of two hydroxyl groups in $[C_3(OH)_2mim][BF_4]$ facilitates the donation of electrons to the hybrid orbitals of the metal ions, leading to formation of well-dispersed small NPs. We also demonstrated an excellent electrocatalytic activity toward H_2O_2 at $[C_3(OH)_2mim][BF_4]$-Au/Pt modified electrode. Herein, a third generation glutamate biosensor based upon $[C_3(OH)_2mim][BF_4]$-Au/Pt film was constructed with glutamate oxidase as the biological recognition element. The mediatorless on-line detection of glutamate was realized at a low potential of −200 mV in the striatum of rat continuously with on-line microdialysis system. The performance of the glutamate biosensor with respect to sensitivity, stability, selectivity, linear range, detection limit and the construction of on-line microdialysis system were presented and discussed in this work. Finally, the prepared biosensor was applied to monitor the variation of glutamate concentration in the striatum stimulated by intraperitoneal (i.p.) injection of 100 mM KCl and electrical stimulation of the subthalamic nucleus area (STN).

2. Experimental

2.1. 2.1Reagents

Glutamate oxidase (GlutaOx; EC 1.4.3.11, 8.0 units/mg), glutamate, ascorbic acid (AA), dopamine (DA), polyethyleneimmine (PEI, 50%, w/v) and Nafion (5 wt%) were purchased from Sigma Co. Artificial cerebrospinal fluid (aCSF: 126 mM NaCl, 2.4 mM KCl, 0.5 mM KH_2PO_4, 0.85 mM $MgCl_2$, 27.5 mM $NaHCO_3$, 0.5 mM Na_2SO_4, 1.1 mM $CaCl_2$, pH 7.4) was prepared with doubly distilled water, filtered (filter pore size 0.22 μm, Millipore, Bedford, MA) and used both as electrolyte for off-line experiment and perfusion solution for on-line measurement. Other reagents were list in Supplementary information.

2.2. Fabrication of GlutaOx-$[C_3(OH)_2mim][BF_4]$-Au/Pt-Nafion biosensor

The screen-printed carbon electrode (3 mm diameter, Zensor R&D, Taichung, Taiwan) and glassy carbon (3 mm diameter, CHI Company, USA) electrode were used in off-line and on-line electrochemical experiments. $[C_3(OH)_2mim][BF_4]$ was synthesized as the Supplementary information and 10 μL of $[C_3(OH)_2mim][BF_4]$ was dispersed in 1.0 mL of 0.5% chitosan solution with the aid of ultrasonic agitation. Then, 5 μL of the mixture was dropped onto the cleaned bare electrode, being allowed to dry at ambient temperature. The electrochemical deposition of Au/Pt NPs was performed in $0.5\,mol\,L^{-1}$ H_2SO_4 aqueous solution containing 0.081 mM of $HAuCl_4$ and 0.16 mM of H_2PtCl_6 at −1.0 V with the time of 50 s. −0.2 V, −0.5 V, −1.0 V, −1.2 V and −1.5 V for the deposition potential were tested through electrochemical methods. The results showed that at −1.0 V, the obtained biosensor displayed the most active electrocatalytic behavior toward H_2O_2. To decrease the size and prevent the aggregation of Au/Pt NPs, the electrodeposition procedure was performed in an ice bath environment with ultrasonic irradiation to the solution. The resulting $[C_3(OH)_2mim][BF_4]$-Au/Pt electrode was carefully rinsed with double-distilled water and dried at room temperature.

For immobilization of GlutaOx onto the $[C_3(OH)_2mim][BF_4]$-Au/Pt modified electrode, 2.0 μL of GlutaOx (8 mg/mL) was mixed with 0.5 μL of 0.4% polyethyleneimide (PEI) solution and then 2.0 μL of the mixture was dropped onto the electrode. PEI was employed here to stabilize the enzyme. After being air-dried for 3 h, the prepared electrode was cross-linked in a closed vessel containing 25% glutaraldehyde and water vapor for 30 min. Finally, 1.0 μL of 2.5% Nafion was dropped onto the electrode to prevent the potential interferences, such as ascorbate acid (AA), dopamine (DA), uric acid (UA), acetaminophen, L-cysteine and other amino acids. The electrode was dried at room temperature for 2 h, and stored at 4 °C until use.

2.3. Instrumentation

The thin layer electrochemical flow cell for the on-line experiments, with an inner volume of 0.085–0.34 μL, consisted of a thin-layer flow block with a 25 μm gasket, GC electrode (3 mm diameter) as working electrode, stainless steel as counter electrode, and saturated calomel electrode as reference electrode and was integrated with microdialysis to form an on-line analytical system for continuous measurement of brain microdialysate of anesthetized rats. Standard solutions or brain microdialysates were delivered from gas-impermeable syringes (BAS) and pumped through a liquid switch (CMA 110, Solna, Sweden) by a microdialysis pump (CMA 402, Solna, Sweden) at a perfusion rate of 2.0 μL/min and determined by the on-line sensors. Other instrumentations can be found in Supplementary information.

2.4. In vivo experimental design

Animal surgical procedures have been depicted in Supplementary information. The *in vivo* experiment was per-

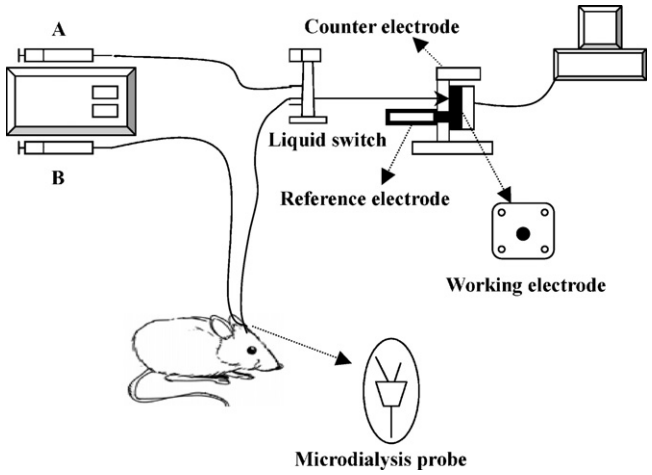

Scheme 1. Schematic presentation of the on-line microdialysis system with GlutaOx modified biosensors for continuous monitoring of glutamate.

formed as previously reported (Yamamoto et al., 2003; Shi et al., 2003) and shown in Scheme 1. Firstly, aCSF solution in syringe A was pumped into the on-line microdialysis system at 2.0 μL/min and flowed to the thin-layer electrochemical flow cell. After a stable baseline was achieved, the syringe selector was switched to syringe B. The current started to increase slowly and then reached a plateau within several minutes, which was ascribed to the biosensing of glutamate in the striatum of rat. Then we switched the selector to syringe A again. Several minutes later, the current response started to decrease and returned to the previous level of background current again.

KCl stimulation was performed by injecting 100 mM KCl intraperitoneally at a dose of 1 mL/kg. Electrical stimulation was delivered via a bipolar stainless steel stimulating electrode insulated everywhere except at the tips. The stimulating electrode was implanted in the subthalamic nucleus area (STN), with a site of 3.5 mm posterior to bregma, 2.4 mm lateral from midline, and 7.0 mm below dura (stimulating parameters: 10 V for 300 s, 0.2 ms, 120 Hz).

Before on-line electrochemical measurements, the microdialysis probes were implanted into the striatum of rats and perfused with aCSF solution at 2.0 μL/min for at least 90 min for equilibration and the injury recovery. The on-line electrochemical biosensor was calibrated with standard solutions of glutamate before and after on-line measurements to ensure there is no obvious change in the sensitivity after the measurements of the brain microdialysis.

2.5. Statistical analysis

Basal level and variation of glutamate concentration in the striatum of rats *in vivo* were expressed as absolute concentrations. Three rats at least were employed for both normal and stimulation experiments. All data were presented as mean ± S.D. ($n = 3$).

3. Results and discussion

3.1. SEM and AFM characterizations of Au/Pt NPs on $[C_3(OH)_2mim][BF_4]$ film

Fig. 1A shows the typical SEM micrograph of the $[C_3(OH)_2mim][BF_4]$-Au/Pt film. It was evident that Au/Pt NPs are well isolated from each other and uniformly distributed on the $[C_3(OH)_2mim][BF_4]$ surface with no agglomeration. The two-dimensional AFM image in Fig. 1B suggests that these Au/Pt NPs reside on the graphite surface as regular spherical-like nanostructures. From the manual analysis (Fig. S1), an average vertical height of 2.5 ± 0.2 nm for Au/Pt NPs was obtained. This value was much smaller than previously reported publications (Xiao et al., 2009; Kang et al., 2007), which may result in a large effective surface area and good electrocatalytic property for the electroactive molecules. We believe that it is the functionalization that facilitates the electron donation from hydroxyl group to the hybrid orbitals of the metal ions, which strengthens the coordination effect between them and leads to the formation of well-dispersed small metal NPs.

3.2. Electrochemical behavior of $[C_3(OH)_2mim][BF_4]$-Au/Pt-Nafion electrode toward H_2O_2

The electrocatalytic activity of $[C_3(OH)_2mim][BF_4]$-Au/Pt-Nafion biosensor toward H_2O_2 reduction was investigated in Fig. 2. Fig. 2A illustrates the cyclic voltammegrams (CV) for bare electrode (a) and $[C_3(OH)_2mim][BF_4]$-Au/Pt-Nafion modified electrode (c) in aCSF (pH 7.4) without (a and c) and with (b and d) 0.5, (e) 2.5, and (f) 6.5 mM H_2O_2 solution at the scan rate of 100 mV s^{-1}. For bare electrode, no catalytic current is observed in 0.5 mM H_2O_2 solution (curves b). On the other hand, with the $[C_3(OH)_2mim][BF_4]$-Au/Pt film electrode, an addition of 0.5 mM H_2O_2 obviously increases the cathodic currents as shown in curve d, which indicates the good electrocatalytical activity of the immobilized $[C_3(OH)_2mim][BF_4]$-Au/Pt film for the reduction of H_2O_2. Moreover, with the successive additions of standard 2.5 and 6.5 mM H_2O_2 solutions (curves e and f), the cathodic currents increase stepwise. The reduction peak potential of about −150 mV herein is more positive than that at reported Ag NPs (−0.68 V vs. SCE) or some reported nanomaterial

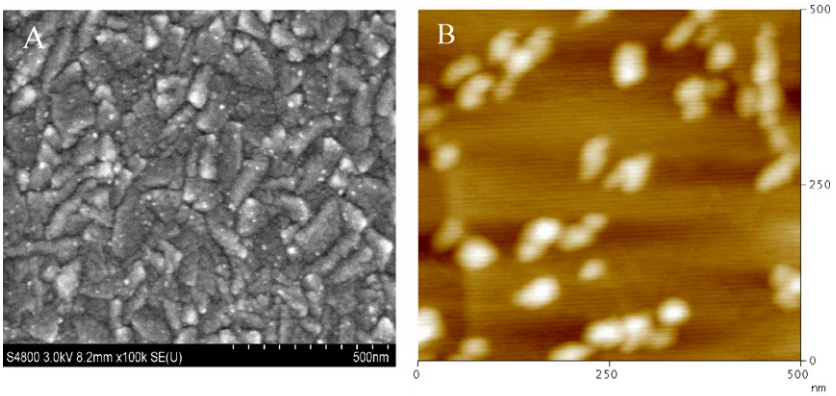

Fig. 1. Typical SEM (A) and AFM (B) images of $[C_3(OH)_2mim][BF_4]$-Au/Pt film.

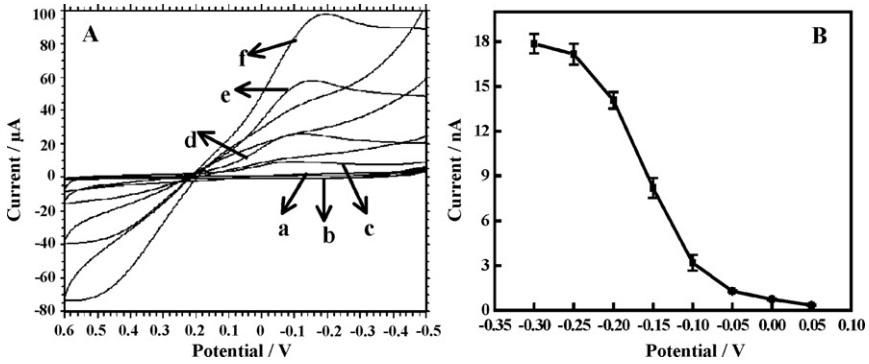

Fig. 2. (A) cyclic voltammograms of (a and b) bare electrode and (c–f) $[C_3(OH)_2mim][BF_4]$-Au/Pt-Nafion modified electrode in (a and c) aCSF blank solution (pH 7.4) and (b and d) 0.5, (e) 2.5 and (f) 6.5 mM H_2O_2 solutions. (B) dependence of the responses of $[C_3(OH)_2mim][BF_4]$-Au/Pt-Nafion electrode to 50 μM H_2O_2 on different working potentials from −300 mV to +50 mV.

modified electrodes (Welch et al., 2005; Wu et al., 2006; Yao et al., 2006), suggesting a faster electron transfer rate toward the reduction of H_2O_2 with our modified $[C_3(OH)_2mim][BF_4]$-Au/Pt-Nafion biosensor. Additionally, as we all know, the typical bioelectrocatalytic reduction of H_2O_2 through the direct electron transfer of HRP normally takes place at ∼−300 mV (vs. Ag/AgCl), introducing great interference from O_2 and AA. The excellent electrocatalytic property of the $[C_3(OH)_2mim][BF_4]$-Au/Pt film is prominent for constituting an analytical protocol for selective determination of H_2O_2.

3.3. Potential and pH-dependence of the responses to H_2O_2 with $[C_3(OH)_2mim][BF_4]$-Au/Pt-Nafion modified electrode

Fig. 2B displays the dependence of amperometric responses of $[C_3(OH)_2mim][BF_4]$-Au/Pt-Nafion biosensor toward 50 μM H_2O_2 on different operating potentials. The currents were measured point by point at each potential from +50 mV to −300 mV. As shown, the amperometric responses increase slightly when the potential ranges from +50 mV to −50 mV. Then it rises sharply from −100 mV to −250 mV. Considering the noise of the background and the interferences from oxygen and AA, −200 mV was selected as the optimal working potential and used in the following electrochemical experiments.

As we will apply the sensor for *in vivo* study, pH 7.4 (the physiological pH value) was selected as the experimental pH, although it may be not the optimal but rather a requirement to detect glutamate *in vivo*. All the subsequent measurements were carried out with aCSF solution (pH 7.4) if not otherwise stated.

3.4. In vitro measurement of glutamate with on-line microdialysis system

The reduction current of glutamate was calibrated *in vitro* with known concentrations of glutamate before the *in vivo* experiments. Fig. 3 is the current responses of different concentrations of glutamate with the on-line microdialysis system *in vitro* at the perfusion rate of 2.0 μL/min. Well-defined steady-state currents are obtained for standard glutamate solutions which are continuously injected into the on-line microdialysis system. The current responses were in good linear with glutamate from 0.5 μM to 20.0 μM (I (nA) = 0.96C (μM) + 1.60, γ = 0.9924) with a sensitivity of 1.60 ± 0.56nA μM^{-1}. The detection limit, based on the signal-to-noise ratio of three, was calculated to be 0.17 μM. This result was much lower than those obtained at redox hydrogel based planar Au electrodes (Castillo et al., 2005) and polypyrrole film based glutamate sensor (Cosnier et al., 1997) and was also comparable to those obtained on poly (amidoamine) dendrimer-encapsulated Pt NPs and MWCNTs modified sensors (Tang et al., 2007a,b).

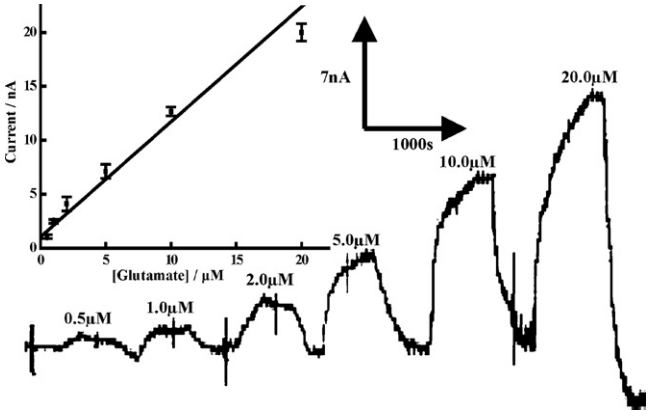

Fig. 3. Amperometric responses of GlutaOx-$[C_3(OH)_2mim][BF_4]$-Au/Pt-Nafion biosensor toward different standard solutions of glutamate in on-line microdialysis system. Inset shows the calibration curve for glutamate from 0.5 μM to 20.0 μM. Flow rate: 2.0 μL/min. Applied potential: −200 mV.

The apparent Michaelis–Menten constant (K_m^{app}), an indication of enzyme–substrate kinetics, can be calculated according to the Lineweaver–Burk equation (Sun et al., 2008). The (K_m^{app}) was calculated to be about 0.033 mM for glutamate, much smaller than previous relative reports (Sun et al., 2008; Liu et al., 2009). This value was also remarkably small as compared to the free GlutaOx, which was 0.21 mM in neutral buffer solution (Kusakabe et al., 1983). The result demonstrates an increased bio-affinity and a higher enzymatic activity toward glutamate with the $[C_3(OH)_2mim][BF_4]$-Au/Pt film modification.

3.5. Selectivity of the GlutaOx-$[C_3(OH)_2mim][BF_4]$-Au/Pt-Nafion biosensor with the microdialysis system

Ascorbic acid (AA) and dopamine (DA) are considered to be the major interferences *in vivo* due to their good electrochemical activity and high concentrations in biological samples (Rahman et al., 2005; Shi et al., 2003). Therefore, the selectivity of GlutaOx-$[C_3(OH)_2mim][BF_4]$-Au/Pt-Nafion biosensor for glutamate determination was evaluated with the on-line microdialysis system. Fig. S2 displays the on-line amperometric responses for 10 μM DA, 0.1 mM AA and 10 μM glutamate at the working potential of −200 mV. The result showed that 0.1 mM of AA and 10 μM of DA cannot produce measurable responses, which convincingly indicates that the measurement of glutamate are essentially interference-free from these electroactive species. It

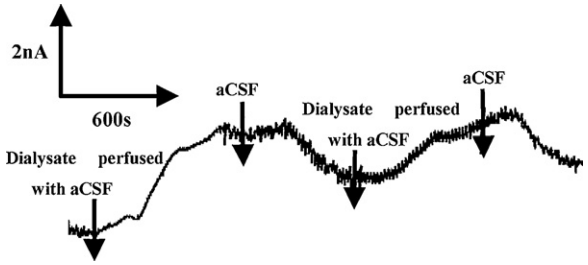

Fig. 4. On-line amperometric responses recorded for glutamate in the striatum of brain dialysate of anesthetic rats repeated for two times in the microdialysis system with the GlutaOx-[$C_3(OH)_2$mim][BF_4]-Au/Pt-Nafion modified electrode. Flow rate: 2.0 μL/min. Applied potential: −200 mV.

was also demonstrated herein that the use of "artificial peroxidase" to replace "natural peroxidase" in the present work, combining with the low operating potential, essentially offers a selective electrochemical method for on-line measurements of biological compounds with *in vivo* microdialysis.

3.6. Reproducibility and stability of the GlutaOx-[$C_3(OH)_2$mim][BF_4]-Au/Pt-Nafion electrode with the on-line microdialysis system

The reproducibility of the method was estimated through consecutively measuring glutamate (10 μM) at the GlutaOx-[$C_3(OH)_2$mim][BF_4]-Au/Pt-Nafion modified electrode with the microdialysis system for 5 times shown in Fig. S3. The RSD value for the amperometric currents (n = 5) was 3.4%, indicating an acceptable fabrication reproducibility under the mentioned conditions.

The stability of the GlutaOx-[$C_3(OH)_2$mim][BF_4]-Au/Pt-Nafion biosensor was checked by employing the biosensor with the on-line microdialysis system for at least 6 days (5–6 h each day). The RSD of current responses to 50 μM glutamate decreased about 4.5%. Moreover, the biosensor retained almost 86% of their initial activity after they were stored at +4 °C for two weeks. The good long-term stability can be ascribed to the excellent biocompatibility of the [$C_3(OH)_2$mim][BF_4]-Au/Pt film, which provides a favorable microenvironment for GlutaOx to maintain its bioactivity.

3.7. In vivo experiments with on-line microdialysis system

After the continuous perfusion for 90 min with aCSF solution, the on-line microdialysis system can start to measure glutamate as Section 2.4 depicted. The relative recovery for glutamate was calculated to be 24% at the flow rate of 2.0 μL/min. For determination of the relative recovery, the probe is immersed in a vial filled with a known concentration of glutamate and then the probe is perfused with aCSF solution at the rate of 2.0 μL/min. The relative recovery is just the ratio as the following equation between the concentration of glutamate which can be calculated from its calibration curve and the known concentration of glutamate in the vial.

$$R(\%) = \frac{C_{out}}{C_{in}} \times 100$$

where R (%) is the relative recovery in percentage, C_{out} is the concentration of the solution calculated from the calibration curve, C_{in} is the known concentration of the solution in the vial.

Fig. 4 displays the current responses recorded for the microdialysate continuously sampled from the striatum of anesthetic rats. The same procedure for *in vivo* experiment was performed two times successively on one rat. There were three rats that were totally investigated. Based on our postcalibration, the basal glutamate concentration in the striatum of rat was calculated to be 3.01 ± 0.67 μM (mean ± S.D., n = 3). This value is comparable to those previously reported using microdialysis (1–4 μM) (Niwa et al., 1996; Shiraishi et al., 1997).

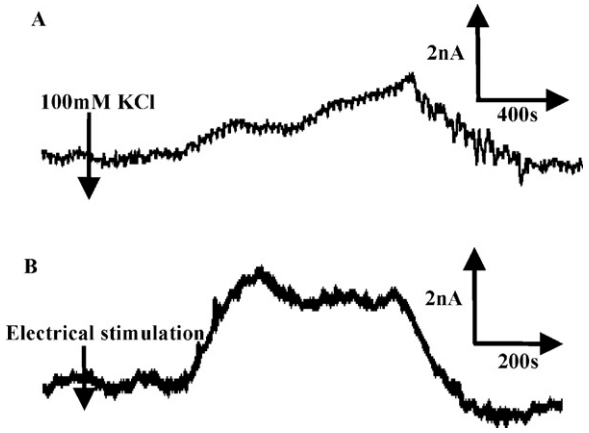

Fig. 5. The variations of glutamate concentration in the striatum caused by injection of 100 mM KCl (A) and electrical stimulation at STN area (B) microdialysis conditions are the same as Fig. 4.

Moreover, to further investigate the possible interference from the electroactive species endogenously existing in the rat brain, glutamate oxidase (0.3 mg/mL) was added to aCSF solution and the mixture was perfused into striatum of rats as some literatures have adopted (Lin et al., 2009; Zhang et al., 2005). No current response was observed under the same conditions, which indicates that the measured catalytic current could be definitely ascribed to glutamate, rather than other interferences (data not shown). It is reasonable that GlutaOx specifically catalyses the oxidation of glutamate in the presence of O_2 and thus the addition of such a kind of oxidase is anticipated to deplete glutamate in the brain microdialysates. These results suggest that the glutamate biosensor is sufficiently sensitive and can detect even the lower basal glutamate levels in the extracellular space of the striatum.

3.8. Variation of glutamate concentration in rat striatum following KCl and electrical stimulation

To investigate whether the biosensor was capable of detecting dynamic change of glutamate in the brain, the influence of exogenous substance administration was studied in this work. Fig. 5A shows the variation in glutamate concentration in the striatum of rat elicited by the injection (i.p.) of aCSF solution containing 100 mM KCl. As can be seen, the response of the dialysate with GlutaOx-[$C_3(OH)_2$mim][BF_4]-Au/Pt–Nafion biosensor increases after KCl injection for 400 s. The increase lasts about 900 s until the current reaches a maximum and then the current response starts to decline and finally returns to the basal level in the striatum. The K^+-stimulated glutamate release in the striatum calculates to be 2.04 ± 0.40 μM (mean ± S.D., n = 3) with respect to the basal level of the extracellular glutamate according to our postcalibration. In addition, to confirm that the response increase was ascribed to the introduction of K^+ rather than the exogenous aCSF solution, an infusion of aCSF solution without KCl in the same dose was also performed. No observable increase in the current response was detected at the GlutaOx-[$C_3(OH)_2$mim][BF_4]-Au/Pt-Nafion biosensor (data not shown). The high concentration of K^+ causes massive depolarization of neurons and consequently, leads to the release of glutamate from vesicular and cytosolic pools. Moreover, the astrocytes may also play a key role in the release of glutamate (Leis et al., 2005; Oldenziel et al., 2006a,b).

We also observed the variation in glutamate concentration following the electrical stimulation at STN. In this experiment,

electrical stimulation was delivered via a bipolar stainless steel stimulating electrode. As Fig. 5B displays, after applying a 10 V potential to the stimulating electrode, the current signal increases and reaches a plateau over a period of 10 min, corresponding to an increase in the striatum glutamate concentration of 4.68 ± 0.30 μM (mean ± S.D., $n = 3$) after postcalibration. After that, the signal decreases and returns to the baseline levels within 200 s. The extracellular glutamate increase induced by electrical stimulation at STN is possibly due to the postsynaptic effects of glutamate receptor activation mediated by various glutamate receptors, which opens Na^+ channels and evokes EPSPs (excitatory postsynaptic potentials). The EPSPs are blocked with specific glutamate antagonists, thus leading to the glutamate release (Lee et al., 2004, 2007). These above results also indicate that the $[C_3(OH)_2mim][BF_4]$-Au/Pt based enzymatic biosensor developed here could be applied to various neurophysiological studies, including the real-time change in the neurotransmitter release or uptake.

4. Conclusions

A new functionalized RTIL, $[C_3(OH)_2mim][BF_4]$, was synthesized and a novel glutamate biosensor based upon $[C_3(OH)_2mim][BF_4]$-Au/Pt film was constructed. The functionalization with hydroxyl group in the imidazolium ring leads to an obvious decrease in the size of Au/Pt NPs. Continuous *in vivo* detection of glutamate was realized integrating with the on-line microdialysis system. Both the normal level and variation of glutamate concentration in the striatum of rats following various stimulations were successfully observed. The results demonstrated that the $[C_3(OH)_2mim][BF_4]$-Au/Pt film, with its low working potential, good sensitivity and selectivity is well suitable for further research *in vivo*.

Acknowledgements

We greatly thank the Program for New Century Excellent Talents in University (NCET-07-0293) and the Science & Technology Commission of Shanghai Municipality (10JC1404000). This work was also supported by the Fundamental Research Funds for the Central Universities and the Funding from Shanghai Key Laboratory of Green Chemistry and Chemical Processes.

Appendix A. Supplementary data

Supplementary data associated with this article can be found, in the online version, at doi:10.1016/j.bios.2010.12.031.

References

Astruc, D., Lu, F., Aranzaes, J.R., 2005. Angew. Chem. Int. Ed. 44, 7852–7872.
Brauer, D.J., Kottsieper, K., Liek, C., Stelzer, O., Waffenschmidt, H., Wasserscheid, P., 2001. J. Organomet. Chem. 630, 177–184.
Castillo, J., Blöchl, A., Dennison, S., Schuhmann, W., Csöregi, E., 2005. Biosens. Bioelectron. 20, 2116–2119.
Chakraborty, S., Raj, C.R., 2007. Electrochem. Commun. 9, 1323–1330.
Cosnier, S., Innocent, C., Allien, L., Poitry, S., Tsacopoulos, M., 1997. Anal. Chem. 69, 968–971.
Daniel, M.C., Astruc, D., 2004. Chem. Rev. 104, 293–346.
Dupont, J., Fonseca, G.S., Umpierre, A.P., Fichtner, P.F.P., Teixeira, S.R., 2002. J. Am. Chem. Soc. 124, 4228–4229.
Fei, Z.F., Zhao, D.B., Pieraccini, D., Ang, W.H., Geldbach, T.J., Scopelliti, R., Chiappe, C., Dyson, P.J., 2007. Organometallics 26 (7), 1588–1598.
Grace, A.A., 1991. Neuroscience 41, 1–24.
Hogant, B.L., Lunte, S.M., 1994. Anal. Chem. 66, 596–602.
Howlett, P.C., MacFarlane, D.R., Hollenkamp, A.F., 2004. Electrochem. Solid State Lett. 7 (5), A97–A101.
Hu, Y., Mitchell, K.M., Albahadily, F.N., Michaelis, E.K., Wilson, G.S., 1994. Brain Res. 659, 117–125.
Itoh, H., Naka, K., Chujo, Y., 2004. J. Am. Chem. Soc. 126 (10), 3026–3027.
Jeffries, C., Pasco, N., Baronian, K., Gorton, L., 1997. Biosens. Bioeletron. 12, 225–232.
Kang, X.H., Mai, Z.B., Zou, X.Y., Cai, P.X., Mo, J.Y., 2007. Anal. Biochem. 369, 71–79.
Kim, K.S., Demberelnyamba, D., Lee, H., 2004. Langmuir 20, 556–560.
Klockgether, T., Turski, L., 1993. Ann. Neurol. 34, 585–593.
Kottsieper, K.W., Stelzer, O., Wasserscheid, P., 2001. J. Mol. Catal. A 175, 285–288.
Kulagina, N.V., Shankar, L., Michael, A.C., 1999. Anal. Chem. 71, 5093–5100.
Kusakabe, H., Midorikawa, Y., Fujishima, T., Kuninaka, A., Yoshino, H., 1983. Agric. Biol. Chem. 47, 1323–1328.
Lee, K.H., Kristic, K., Hoff, R.V., Hitti, F.L., Blaha, C., Harris, B., Roberts, D.W., Leiter, J.C., 2007. Brain Res. 1162, 121–129.
Lee, K.H., Chang, S.Y., Roberts, D.W., Kim, U., 2004. J. Neurosurg. 110, 511–517.
Leis, J.A., Bekar, L.K., Walz, W., 2005. Glia 50, 407–416.
Lin, Y.Q., Zhu, N.N., Yu, P., Su, L., 2009. Anal. Chem. 81, 2067–2074.
Liu, M.C., Zhao, G.H., Zhao, K.J., Tong, X.L., Tang, Y.T., 2009. Electrochem. Commun. 11, 1397–1400.
Maciej, G.N., Andrzej, L., Izabela, S.E., 2006. Electrochim. Acta 51, 5567–5580.
Mao, L.Q., Yamamoto, K., 2000. Talanta 51, 187–195.
Niwa, O., Horiuchi, T., Torimitsu, K., 1997. Biosens. Bioelectron. 12, 311–319.
Niwa, O., Torimitsu, K., Morita, M., Osborne, P., Yamamoto, K., 1996. Anal. Chem. 68, 1865–1870.
Oldenziel, W.H., Dijkstra, G., Cremers, T.I.F.H., Westerink, B.H.C., 2006a. Brain Res. 1118, 34–42.
Oldenziel, W.H., Dijkstra, G., Cremers, T.I.F.H., Westerink, B.H.C., 2006b. Anal. Chem. 78, 3366–3378.
Rahman, M.A., Kwon, N.H., Won, M.S., Choe, E.S., Shim, Y.B., 2005. Anal. Chem. 77, 4854–4860.
Shi, G.Y., Yamamoto, K., Zhou, T.S., Xu, F., Kato, T., Jin, J.Y., Jin, L.T., 2003. Electrophoresis 24, 3266–3272.
Shiraishi, M., Kamiyama, Y., Huttemeier, P.C., Benveniste, H., 1997. Brain Res. 759, 221–227.
Sun, Z.Y., Li, Y.Q., Zhou, T.S., Liu, Y., Shi, G.Y., Jin, L.T., 2008. Talanta 74, 1692–1698.
Tang, L.H., Zhu, Y.H., Yang, X.L., Li, C.Z., 2007a. Anal. Chim. Acta 597, 145–150.
Tang, L.H., Zhu, Y.H., Xu, L.H., Yang, X.L., Li, C.Z., 2007b. Talanta 73, 438–443.
Tian, Y., Liu, H.Q., Zhao, G.H., Tatsuma, T., 2006. J. Phys. Chem. B 110, 23478–23481.
Tong, Q., Ye, C., McCrimmon, R.J., Dhillon, H., Choi, B., Kramer, M.D., Yu, J., Yang, Z., Christiansen, L.M., Lee, C.E., Choi, C.S., Zigman, J.M., Shulman, G.I., Sherwin, R.S., Elmquist, J.K., Lowell, B.B., 2007. Cell Metab. 5, 383–393.
Wang, P., Zakeeruddin, S.M., Moser, J.E., Gratzel, M., 2003. J. Phys. Chem. B 107, 13280–13285.
Weite, H.O., Ben, H.C., Westerink, 2005. Anal. Chem. 77, 5520–5528.
Welch, C.M., Banks, C.E., Simm, A.O., Compton, R.G., 2005. Anal. Bioanal. Chem. 382, 12–21.
Whitehead, J.A., Lawrance, G.A., McCluskey, A., 2004. Green Chem. 6, 313–315.
Wilson, G.S., Johnson, M.A., 2008. Chem. Rev. 108, 2462–2481.
Wu, S., Zhao, H.T., Ju, H.X., Shi, C.G., Zhao, J.W., 2006. Electrochem. Commun. 8, 1197–1203.
Xiao, F., Zhao, F.Q., Zhang, Y.F., Guo, G.P., Zeng, B.Z., 2009. J. Phys. Chem. C 113, 849–855.
Yamamoto, K., Shi, G.Y., Zhou, T.S., Xu, F., Xu, J.M., Kato, T., Jin, J.Y., Jin, L.T., 2003. Analyst 128, 249–254.
Yao, S.J., Xu, J.H., Wang, Y., Chen, X.X., Xu, Y.X., Hu, S.H., 2006. Anal. Chim. Acta 557, 78–84.
Zhang, H., Li, Z.P., Zhang, J., Zhang, S.G., Zhu, L.Y., Yang, J., Zhang, X.P., Deng, Y.Q., 2007. J. Phys. Chem. B 111, 2864–2872.
Zhang, M.N., Liu, K., Gong, K.P., Su, L., Chen, Y., Mao, L.Q., 2005. Anal. Chem. 77 (19), 6234–6242.